

Atomistic analysis of defect evolution and transient enhanced diffusion in silicon

Maria Aboy,^{a)} Lourdes Pelaz, Luis A. Marqués, L. Enriquez, and Juan Barbolla
University of Valladolid, Campus Miguel Delibes s/n, 47011 Valladolid, Spain

(Received 28 October 2002; accepted 6 May 2003)

Kinetic Monte Carlo simulations are used to analyze the ripening and dissolution of small Si interstitial clusters and {113} defects, and its influence on transient enhanced diffusion of dopants in silicon. The evolution of Si interstitial defects is studied in terms of the probabilities of emitted Si interstitials being recaptured by other defects or in turn being annihilated at the surface. These two probabilities are related to the average distance among defects and their distance to the surface, respectively. During the initial stages of the defect ripening, when the defect concentration is high enough and the distance among them is small, Si interstitials are mostly exchanged among defects with a minimal loss of them to the surface. Only when defects grow to large sizes and their concentration decreases, the loss of Si interstitials through diffusion to the surface prevails, causing their dissolution. The presence of large and stable defects near the surface is also possible when the implant energy is low—small distance to the surface—but the dose is high enough—even smaller distance among defects. The exchange of Si interstitials among defects sets a interstitial supersaturation responsible for the temporary enhancement of the diffusivity of interstitial diffusing dopants. The transitory feature of the enhancement is well correlated to the extinction of the Si interstitial defects. © 2003 American Institute of Physics. [DOI: 10.1063/1.1586990]

I. INTRODUCTION

Ion implantation is the standard method to introduce dopants in silicon for the fabrication of integrated circuits. However, this process produces considerable damage in the Si lattice due to the energetic collisions of ions with the host atoms. The defects generated in this way might degrade the device characteristics and thus, a postimplant thermal process is necessary to anneal out the damage. Frenkel pairs generated in each implantation cascade are annealed out quickly and only Si interstitials generated by the implanted ions survive. The excess of Si interstitials that remains from the implanted ions (“+1” model¹) condense into Si interstitial clusters, {113} defects, and dislocation loops.^{2–6} These defects sustain a local supersaturation of Si interstitials by emitting and recapturing interstitials during annealing. The presence of the Si interstitial supersaturation causes transient enhanced diffusion (TED) in interstitial diffusing dopant atoms. The transitory character of TED is associated to the extinction of the reservoir of Si interstitials, as the interstitials are gradually lost from the damage region through diffusion to the surface. For medium implant doses and energies, {113} defects are found to be the main source of interstitials for TED.⁵ For low implant doses or in the presence of high boron concentrations, TED has been monitored, even in the absence of {113} defects.^{7,8} In these cases, small Si interstitial clusters or boron–interstitial clusters are considered to be the reservoir of Si interstitials which cause TED. However, even in those cases in which {113} defects are observed, many controversies are found in the literature about the role

of the surface in the interstitial removal from {113} defects and about the correlation between TED and {113} defects.^{9–13}

The role of the silicon surface in the removal of point defects has been investigated by Lim *et al.*⁹ These authors have shifted the position of the surface in relation to the damage by the use of chemical etching. Their results indicated that surface proximity reduces TED and the surface behaves as an efficient sink for Si interstitials. Venezia *et al.*¹⁰ have observed, also by using chemical etching, a linear dependence of the dissolution time of the {113} defects with depth. They concluded that {113} dissolution is controlled by surface annihilation in analogy to TED. The role of the surface in ultrashallow junctions (ultralow energy) has been investigated by Agarwal *et al.*¹¹ They have shown that despite the proximity to the surface, large and stable {113} defects are observed even for 5 keV Si implants. Moller *et al.*¹² suggested that surface is not the limiting factor in the interstitial removal from {113} defects during the annealing, since the defect layer does not exhibit preferential annihilation closer to the surface. They showed that the {113} defects dissolve uniformly across the layer, and the width of the layer does not change until the {113} defects nearly completely dissolve. Saleh *et al.*¹³ claimed no correlation between TED and {113} dissolution since TED depends strongly on implant energy but the {113} dissolution is weakly dependent.

In this article, we study by atomistic simulation techniques the influence of the surface in Si interstitial defect dissolution and TED. We provide a comprehensive understanding of the different results reported in the literature and explain the apparent contradictions that appear in the experiments. Experimental techniques, such as transmission elec-

^{a)} Author to whom correspondence should be addressed; electronic mail: marabo@tel.uva.es

tron microscopy, used to observe defects in silicon, can only capture the presence of defects of relatively large size, such as $\{113\}$ defects or dislocation loops. Other small defects may exist in Si samples that are not seen in the experiments. In the simulations we account for interstitial defects of any size, including small clusters.

II. PHYSICAL MODELING

For our study, we carried out atomistic simulations with the following scheme: implantation cascades are simulated with the binary collision computer code MARLOWE,¹⁴ and the coordinates of the resulting Si self-interstitials and vacancies are transferred to the kinetic nonlattice Monte Carlo diffusion code DADOS.¹⁵ In the nonlattice kinetic Monte Carlo technique, only the atoms belonging to point or extended defects are simulated. Clusters of point defects are formed when the mobile point defects jump within the capture radius of other point defects or pre-existing clusters. We consider that defects interact when they are within second-neighbor distance of each other. The dissolution of the defects occurs by the emission of a point defect at a rate determined by their binding energy. The energies used in Monte Carlo simulations are obtained from *ab initio* calculations or estimated by fitting experimental data.^{5,6} The migration and formation energies for Si self-interstitials are taken from Ref. 16. For small Si interstitial clusters ($n < 10$) we take the oscillating formation energies experimentally deduced by Cowern *et al.*⁶ For larger sizes, we use an expression¹⁷ that tends asymptotically to the experimental binding energy of $\{113\}$ defects.^{6,18} No loops are formed in the experiments under study. The surface is considered as an efficient sink for point defects, with a recombination length $L \leq 20$ nm.^{9,19,20}

III. SIMULATION RESULTS AND DISCUSSION

A. Spatial and temporal evolution of a layer of $\{113\}$ defects

We have investigated the role of the surface in the removal of Si interstitials from the top and the bottom of a layer of $\{113\}$ defects by analyzing the time evolution of the Si interstitial defects. We simulate the implantation of 40 keV Si ions, to a dose of 10^{14} ions/cm² with a dose rate of 10^{12} ions/cm² s, followed by an anneal at 750 °C for up to 15 000 s, as in the experiment by Moller *et al.*¹² Figure 1 shows the simulated time evolution of the dose of silicon interstitials, the dose of the defects, and the mean size of these defects.

Several stages can be distinguished in the temporal evolution of damage during the postimplant anneal. During the ramp up, and at the very early stages of the anneal, there is a high concentration of Si interstitials and also a high concentration of vacancies generated by the implantation. Interstitials and vacancies recombine quickly, leaving approximately one Si interstitial per implanted ion which cannot be annealed out with the corresponding vacancies (dose $\sim 10^{14}$ cm⁻²). As the anneal proceeds, the “+1” interstitials condense into small interstitial clusters and $\{113\}$ defects. At 750 °C the evolution from small clusters ($n < 20$) to bigger sizes occurs very rapidly. After 40 s, 90% of the defects are

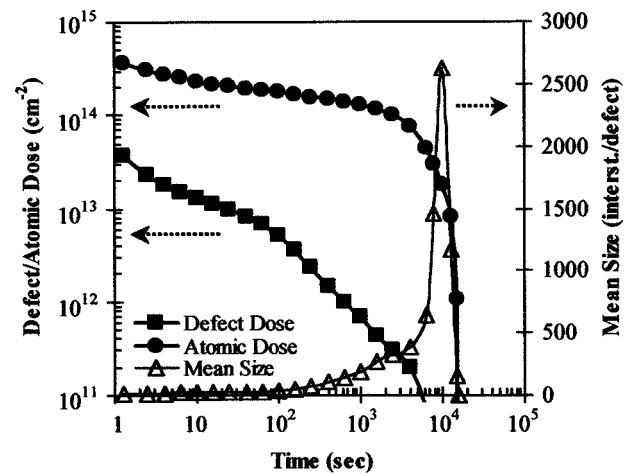


FIG. 1. Time evolution during annealing at 750 °C of the atomic and defect dose of Si interstitials in defects for a simulated 40 keV Si implant to a dose of 10^{14} ions/cm² with a dose rate of 10^{12} ions/cm² s. Time evolution of the mean size of the defects is also plotted.

already clusters with more than 20 atoms, and a small fraction survives mostly as eight-interstitial clusters, which is considered very stable in the model.⁶ During a long period of time (~ 6000 s), the interstitial dose remains almost constant ($\sim 10^{14}$ cm⁻²) as very few interstitials are lost to the surface. During this period of time, the mean size of the defects increases by the exchange of Si interstitials among them, at the same time that the defect dose decreases. Once the mean size of the defects has reached a large value, and the defect dose is low, the Si interstitial dose held in the defects decreases quickly as many Si interstitials are lost through diffusion to the surface.

In Fig. 2 we have plotted the simulated depth profiles of the Si interstitial concentration, as-implanted and after annealing at 750 °C for 10, 1000, 6000, and 8000 s. The depth profile of vacancies after 10 s anneal is also plotted. The

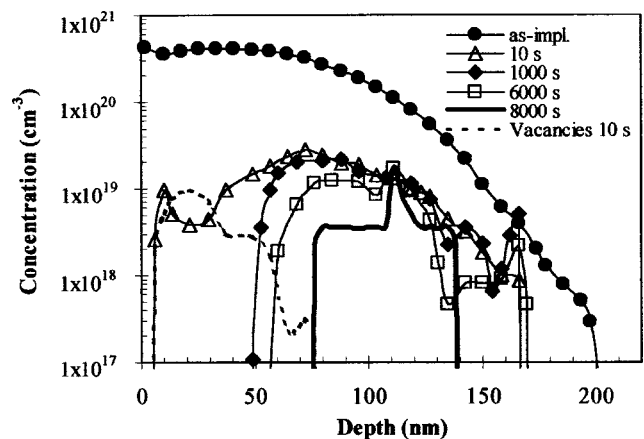


FIG. 2. Simulated Si interstitial and vacancy depth profiles obtained from different times during the annealing at 750 °C of a 10^{14} cm⁻², 40 keV Si implant. The as-implanted profile of vacancies overlaps with the one for Si interstitials. The reduction in Si interstitials is fast while there are vacancies present, due to recombination. The profile does not change considerably from 1000 to 6000 s. The dissolution of defects takes place from both sides of the defect layer, as can be seen in the profile at 8000 s compared with the one for 6000 s.

as-implanted profile for vacancies overlaps with the one for Si interstitials. The figure shows that initially there is a fast reduction in the Si interstitial concentration, mainly due to the presence of the vacancies. At 10 s there is still a significant concentration of vacancies near the surface causing the recombination of the Si interstitials in this region. Once the vacancies are completely annealed out, the decrease in Si interstitial concentration only occurs by annihilation at the surface, which is minimal at the beginning of the anneal. From about 1000 to 6000 s the Si interstitial concentration profile does not change significantly, while the average defect size increases significantly (see Fig. 1). However, as we previously mentioned, there is a fast decrease in the interstitial concentration from 6000 to 8000 s.

This could be explained by the random-walk theory.²¹ At the first stages of the anneal, when there are many small defects, the distance among them is much shorter than the distance to the surface. Therefore, interstitials are more likely to be recaptured by another defect than to reach the surface. In this way, Si interstitials are emitted from and recaptured by clusters, favoring the growth of larger and more stable defects at the expense of smaller ones (Ostwald ripening). As the average size of the defects increases during the ripening, the density of defects decreases, in order to keep approximately constant the density of Si interstitials,

$$\text{Atomic_Dose} = \text{Defect_Dose} \times \text{Mean_Size}. \quad (1)$$

Therefore, the average distance among the defects, d_{def} , increases as the defect dose decreases, since the mean distance among defects can be estimated by

$$d_{\text{def}} = \sqrt[3]{\frac{(d_{\text{max}} - d_{\text{min}})}{\text{Defect_Dose}}}, \quad (2)$$

where $d_{\text{max}} - d_{\text{min}}$ is the width of the defect layer. Then, when the distance among defects becomes comparable to the distance to the surface, the probability of interstitials being recaptured in the layer becomes comparable to the probability of them being annihilated at the surface. At this point, as the exchange of interstitials continues, a significant number of Si interstitials are lost by recombination at the surface. The defect dose decreases further, the distance among defects increases, and consequently the probability of interstitials being annihilated at the surface increases. This results in the quick dissolution of Si interstitial defects at the final stages of the anneal.

The experiments by Moller *et al.*¹² showed that the position of the top and the bottom of the {113} layer does not change considerably until the {113} defects nearly completely dissolve, and the position of the bottom of the {113} layer does not exhibit preferential annihilation. They suggested that defect dissolution does not appear to be controlled by the surface annihilation. Our simulations show similar results when the surface is considered as an efficient sink for point defects ($L = 10$ nm). Figure 3 shows the simulated time evolution of the top and the bottom depth of the Si interstitial layer, and the experimental results reported by Moller *et al.*¹² The figure shows that the defect layer remains almost unchanged for about 6000 s. This instant corresponds

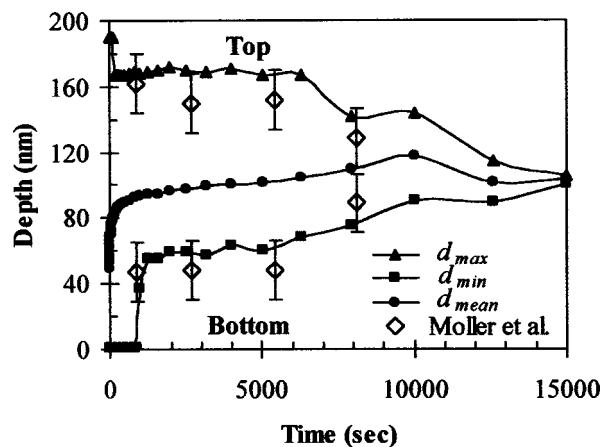


FIG. 3. Time evolution of the top (d_{max}), the bottom (d_{min}), and the mean (d_{mean}) position of the Si interstitials in the defect layer. Experimental data from Moller *et al.* (Ref. 12) are also plotted. The d_{max} and d_{min} positions are kept approximately constant up to 6000 s. At 8000 s the defect layer shrinks from both sides. Note that the mean position of the Si interstitials slowly shifts towards deeper positions.

in the simulation to a defect dose of about $7 \times 10^{10} \text{ cm}^{-2}$ and a defect layer width of 100 nm. The estimated mean distance among defects is then about 50 nm, which is comparable to the distance of the defect layer to the surface. Then, there is a no negligible probability of a Si interstitial, even from the top region, to go through the layer and to reach the surface, and both sides of the defect layer shrink. Nevertheless, note that the mean position slightly shifts towards deeper positions. Therefore, the results reported by Moller *et al.* are compatible with the fact that the surface controls the dissolution of {113} defects.

The Si interstitial defect dissolution and the conclusion of TED are due to the annihilation of Si interstitials through diffusion to the surface. We study TED in terms of the time integrated interstitial supersaturation, which is proportional to the diffusivity enhancement of interstitially diffuser dopant atoms. The time integrated interstitial supersaturation for the 40 keV Si implant to a dose of 10^{14} cm^{-2} , then annealed at 750 °C, is plotted in Fig. 4. As we have seen previously, during the first 4000 s of the anneal the loss of Si interstitials to the surface is very small. However, approximately half the total amount of TED is reached by 4000 s, before the significant loss of Si interstitials to the surface. During this period of time there is an exchange of interstitials among defects, leading to the ripening of the defects to larger sizes and causing a Si interstitial supersaturation in the surrounding regions. These free Si interstitials can interact with dopants and thus, cause TED. Initially, the Si interstitial supersaturation is large (high slope in Fig. 4 at the beginning of the anneal), as corresponds to the ripening of the small and unstable Si interstitial clusters.^{6,8} Although the interstitial supersaturation set by unstable clusters is very high, the time of existence of these small clusters is very short (< 40 s). Therefore, its contribution to the total diffusivity enhancement is small (see Fig. 4). During the rest of the annealing time, there is an approximately constant and lower Si interstitial supersaturation, which is set by more stable clusters and {113} defects with binding energies of 2.6–2.8 eV. Finally,

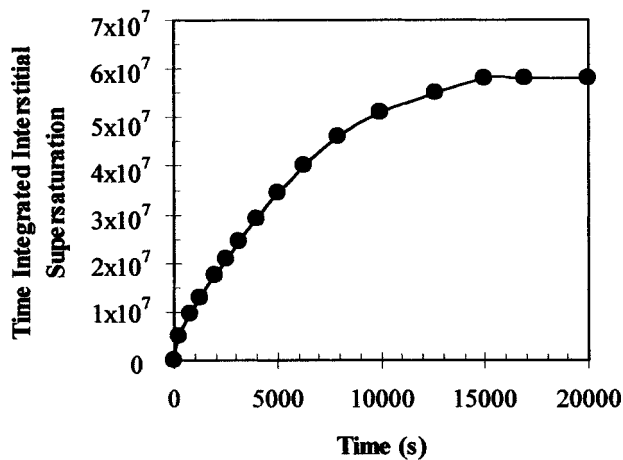


FIG. 4. Time evolution of the time integrated interstitial supersaturation for a 40 keV Si implant to a dose of 10^{14} cm^{-2} during annealing at 750°C . Approximately half the total time integrated interstitial supersaturation (which is proportional to the total amount of TED) is reached during the initial 4000 s.

when the reservoir of Si interstitials extinguishes, the curve flattens.

Saleh *et al.*¹³ varied the distance to the surface, with implantation energies from 20 to 160 keV, and measured the characteristic time constants for TED (by measuring the junction depth broadening of a boron marker layer and assuming an exponential decay in diffusivity with time) and $\{113\}$ defect dissolution (measured from the slope of the fast decay region of the Si interstitial dose in $\{113\}$ defects versus time). They observed that while the characteristic time for TED clearly increases with the implanted energy–distance to the surface, the characteristic time for $\{113\}$ defect dissolution varies very weakly with the implanted energy. The divergence between these two times is more significant at higher energies. Therefore, they concluded that there is no correlation between the characteristic time constants for TED and $\{113\}$ defect dissolution. The diffusivity enhancement occurs due to the presence of a Si interstitial supersaturation. This situation exists not only during the period of time when there is a considerable loss of Si interstitials (which corresponds to the measured $\{113\}$ dissolution time), but also during the defect ripening. Therefore, it would be more precise to have the correlation between the duration of the transitory diffusivity enhancement and the total time of existence of any source of Si interstitials. In the case under study, most of the Si interstitials agglomerates into $\{113\}$ defects, and they can be considered the main source of Si interstitials. The time before the onset of $\{113\}$ dissolution, t_{on} (the almost flat region in Fig. 1, and also in Saleh's experiments), cannot be neglected because during this time there is an exchange of interstitials among defects that sets an interstitial supersaturation responsible for a significant fraction of the total TED (as it is shown in Fig. 4). Thus, for the 160 keV implant, the extracted value for the dissolution time constant is $\tau_s = 43$ min, while the time before the onset of dissolution is $t_{\text{on}} = 75$ min. This time is larger for higher implant energies: larger distances to the surface allow more exchange of Si interstitials among defects before a significant loss of them

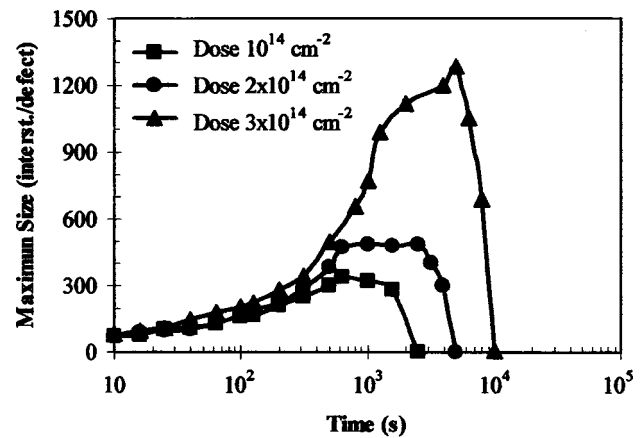


FIG. 5. Time evolution of the maximum size of defects for 5 keV Si implants with implantation doses from 10^{14} to $3 \times 10^{14} \text{ cm}^{-2}$, annealed at 750°C . A sharp increase in the maximum size is observed when going from 2×10^{14} to $3 \times 10^{14} \text{ cm}^{-2}$.

occurs by surface annihilation. For low energies, t_{on} is very short, and the experimentally measurable times correspond already to the dissolution stage. For this reason, the divergence in the calculated time constants for TED and $\{113\}$ dissolution is larger at higher energies. Using the values reported in the experiments of Ref. 13, when the time constants for TED are compared with the time constant of $\{113\}$ defects (including the time before the onset of dissolution), the values are well correlated.

B. $\{113\}$ defects from low energy and high dose implants

Another apparent contradiction to the fact that the surface controls the dissolution of the $\{113\}$ defects is the observation of large and very stable clusters near the surface for low energy and high dose implants.¹¹ For a 5 keV Si implant followed by an anneal at 750°C , the formation of $\{113\}$ defects is seen in the experiments in spite of the proximity to the surface. Moreover, a superlinear increase in their size and stability is observed when going from implantation doses of 10^{14} – $3 \times 10^{14} \text{ ions/cm}^2$.

The simulation results show similar behavior, as can be seen in Fig. 5, where we plot the maximum defect size for 5 keV Si implants with doses of 10^{14} , 2×10^{14} , and $3 \times 10^{14} \text{ ions/cm}^2$, and annealed at 750°C . In spite of the proximity to the surface for the low energy implants, we obtain large and very stable clusters for the high implant dose. The defect size increases with implantation dose, with a large rise in size when going from 2×10^{14} to $3 \times 10^{14} \text{ ions/cm}^2$. The formation of these long and stable defects is related to the high concentration of excess interstitials that appears for the high dose implants. This leads to a significant reduction in the average distance among defects within the defect layer. Therefore, interstitials emitted from defects in the layer are likely to be recaptured despite the proximity to the surface, and large defects can be formed. These large and stable defects could be the zig-zag $\{113\}$ defects showed by Agarwal *et al.*¹¹ We obtain a superlinear

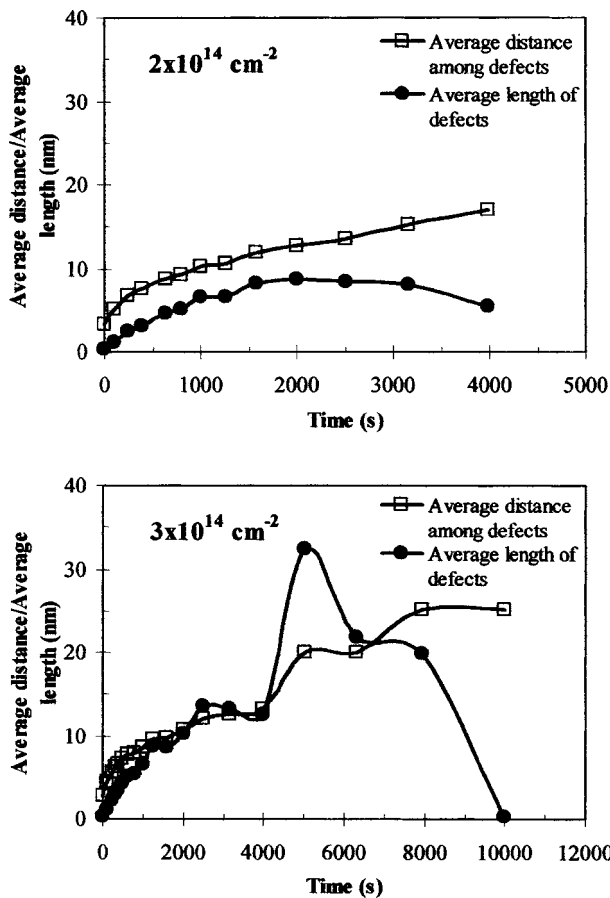


FIG. 6. Time evolution of the average distance among defects and average length of defects, extracted from the simulations of 5 keV implants with implantation doses of: (top) $2 \times 10^{14} \text{ cm}^{-2}$ and (bottom) $3 \times 10^{14} \text{ cm}^{-2}$, and annealed at 750°C . In the lower dose case, the average distance among defects is always smaller than the average length of the defects, while in the higher dose case, the average length of the defects can be even larger than the average distance among defects.

increase in the duration of Si interstitial defects with the implantation dose, as is observed in the experiments too.

So far, we have considered the formation and dissolution of the defects in terms of a competition between the average distance among defects and the distance to the surface. However, this do not explain the superlinearity with ion implantation dose that appears in the size and stability of the defects. The dissolution time and size of the defects is expected to have a linear dependence with dose according to Ref. 22 and Eq. (1). To explain the anomalous behavior observed for the $3 \times 10^{14} \text{ ions/cm}^2$, 5 keV Si implant, we have analyzed in more detail the ripening of the defects formed during annealing. The average distance among defects is estimated using Eq. (2), with Defect_Dose and $d_{\text{max}} - d_{\text{min}}$ extracted from the simulations. The average length of the defects is extracted from the Mean_Size (average number of interstitials per defect) given by the simulations, using an average number of 25 interstitials per nm of length.²³ The time evolution of both magnitudes for the 2×10^{14} and the $3 \times 10^{14} \text{ ions/cm}^2$ doses, respectively, is plotted in Figs. 6(a) and 6(b). For the $10^{14} \text{ ions/cm}^2$ case, the obtained evolution is similar to the one for the $2 \times 10^{14} \text{ ions/cm}^2$ case, but the average length of the defects is even smaller. For the low dose case, the length

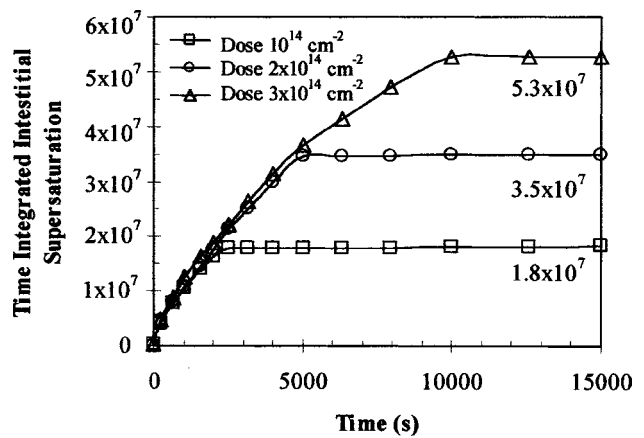


FIG. 7. Evolution of the time integrated interstitial supersaturation for 5 keV Si implants with implantation doses ranging from 10^{14} to $3 \times 10^{14} \text{ cm}^{-2}$ during annealing at 750°C . The duration of TED (time until the curve becomes flat), increases superlinearly with the implantation dose, but this is accompanied by a reduction in the Si interstitial supersaturation (slope). Thus, the total time integrated interstitial supersaturation (and so, TED) is approximately proportional to the implantation dose.

of the defects is smaller than both the distance to the surface ($\sim 10 \text{ nm}$) and the distance among defects, during all the annealing time. However, for the high dose case, the size of the defects becomes such that their average length can even be larger than the average distance among defects. This could lead to an interaction between $\{113\}$ defects with different orientations to form longer and thicker defects, and the zig-zag structures.¹¹

The stability of long clusters and their larger capture radius favors the recapture of the emitted Si interstitials. This sets a reduced Si interstitial supersaturation, and hence, a smaller flux of Si interstitials to the surface, resulting in a slower dissolution of the defects. Its influence on TED can be seen in Fig. 7, where we plot the evolution of the time integrated interstitial supersaturation for the $10^{14} - 3 \times 10^{14} \text{ cm}^{-2}$, 5 keV Si implants during the annealing at 750°C . As can be seen, the duration of TED (time until the curve flattens), increases superlinearly with dose, but the increase in time is accompanied by a decrease in the effective interstitial supersaturation (reduction in the slope in Fig. 7). As a result, the total amount of TED total time integrated interstitial supersaturation

$$\left(\int_0^{t_{\text{final}}} \frac{C_I}{C_I^*} dt \right)$$

is approximately proportional to the dose at the end of the transient. According to the model proposed by Rafferty et al.,²² the free Si interstitial supersaturation, C_I/C_I^* , in local equilibrium with defects of binding energy E_b , has an activation energy given by $(-E_b + E_f)$, E_f being the formation energy of the Si self-interstitial from the ground state. On the other hand, the total time to dissolve the Si interstitial defects, and therefore to finish TED, t_{TED} , has an activation energy given by $(E_b + E_m)$, E_m being the migration energy of the Si self-interstitial. This implies that stable defects (larger E_b) cause a lower supersaturation but subsist for longer time, and vice versa, unstable defects set a high su-

persaturation for a short time. The TED to completion is given approximately by $C_I/C_I^*t_{\text{TED}}$, which corresponds to an activation energy given by $(E_f + E_m)$, independent on the binding energy of the Si interstitial defects.²⁴

Analogous reasoning can be done from an atomistic point of view: TED is proportional to the number of times that a Si interstitial visits a lattice position and, therefore, it can interact with a dopant atom in that position. From the random-walk theory,²⁰ the average number of hops, N , of a Si interstitial in its way to the surface, only depends on the distance to the surface,²⁵ D , and the jump distance, λ , according to $N = (D/\lambda)^2$. The temporary trapping of the Si interstitials in immobile defects only delays their arrival to the surface. If intermediate stages were monitored, the number of hops until that instant would depend on the stability of the defects, as they determine the number of free Si interstitials in each instant. However, the total number of hops to completion is independent of the stability of the Si interstitial defects, as it only depends on the amount of Si interstitials and their distance to the sink. In fact, the scenario after an implant is more complicated because vacancies also act as a sink for Si interstitials. The large number of Si interstitials generated during ion implantation gives some hops before its recombination with vacancies. There is one interstitial per implanted ion that does not have the corresponding vacancy to recombine with, and has to diffuse to the surface to be annihilated. In most cases, the number of hops given by Frenkel pairs before its recombination is negligible compared to the contribution of the excess interstitials, giving validity to the “+1 model.”²⁶ In some cases, the incomplete recombination of Frenkel pairs causes that the effective number of Si interstitials diffusing to the surface to deviate from the “+1,” giving rise to more complex dependences with the implant parameters.²⁷

IV. CONCLUSIONS

We have used atomistic kinetic Monte Carlo techniques to analyze the interstitial defect evolution and its correlation with TED. We have shown that the defect dissolution during the postimplant annealing is controlled by the annihilation of Si interstitials at the surface. This is compatible with experiments, which indicates that both sides of a {113} layer does not change considerably until the defects nearly completely dissolve, and the position of the bottom of the {113} layer does not exhibit preferential annihilation. Also, the formation of stable defects close to the surface in low energy implants is possible if the implantation dose is high enough.

The ripening and dissolution of Si interstitial defects can be explained as a competition between the surface and other defects to capture the emitted Si interstitials. Initially, the exchange of interstitials among defects dominates the process, leading to the formation of larger defects at the expense of the smaller ones, with a minimal loss of the total number of Si interstitials. As the defect dose decreases and their size increases, the average distance among them increases. Then, the role of the surface, in terms of interstitial annihilation,

becomes more important. The use of low energy and high dose implants results in a reduction of both the distance of the defects to the surface and the average distance among them. Thus, it is possible that there is formation of large interstitial defects close to the surface. If the dose is high enough, defects may become so large that their length can be even longer than the distance among them. This makes the recapture of Si interstitials by defects very efficient and slows down its dissolution. In all cases, the time of existence of Si interstitial defects and the duration of TED are clearly correlated, as TED is caused by Si interstitials released from Si interstitial defects.

¹M. Giles, *J. Electrochem. Soc.* **138**, 1160 (1991).

²P. A. Stolk, H.-J. Gossmann, D. J. Eaglesham, D. C. Jacobson, C. S. Rafferty, G. H. Gilmer, M. Jaraiz, J. M. Poate, H. S. Luftman, and T. E. Haynes, *J. Appl. Phys.* **81**, 6031 (1997).

³K. S. Jones, J. Chen, S. Bharatan, J. Jackson, L. Rubin, M. Puga-Lambers, and D. Venables, *J. Electron. Mater.* **26**, 1361 (1997).

⁴M. Jaraiz, G. H. Gilmer, J. M. Poate, and T. D. De la Rubia, *Appl. Phys. Lett.* **68**, 409 (1996).

⁵D. J. Eaglesham, P. A. Stolk, H.-J. Gossmann, and J. M. Poate, *Appl. Phys. Lett.* **65**, 2305 (1994).

⁶N. E. B. Cowern *et al.*, *Phys. Rev. Lett.* **82**, 4460 (1999).

⁷L. H. Zhang, K. S. Jones, P. H. Chi, and D. S. Simons, *Appl. Phys. Lett.* **67**, 2025 (1995).

⁸H. G. A. Huizing, C. G. G. Visser, N. E. B. Cowern, P. A. Stolk, and R. C. M. de Kruij, *Appl. Phys. Lett.* **69**, 1211 (1996).

⁹D. R. Lim, C. S. Rafferty, and F. P. Klemens, *Appl. Phys. Lett.* **67**, 2302 (1995).

¹⁰V. C. Venezia, R. Kalyanaraman, H.-J. Gossmann, C. S. Rafferty, and P. Werner, *Appl. Phys. Lett.* **79**, 1429 (2001).

¹¹A. Agarwal, H.-J. Gossmann, D. J. Eaglesham, L. Pelaz, S. B. Herner, D. C. Jacobson, T. E. Haynes, and R. Simonton, *Mater. Sci. Semicond. Process.* **1**, 17 (1998).

¹²K. Moller, K. S. Jones, and M. E. Law, *Appl. Phys. Lett.* **72**, 2547 (1998).

¹³H. Saleh, M. E. Law, S. Bharatan, K. S. Jones, V. Krishnamoorthy, and T. Buyuklimanli, *Appl. Phys. Lett.* **77**, 112 (2000).

¹⁴M. T. Robinson and I. M. Torrens, *Phys. Rev. B* **9**, 5008 (1974).

¹⁵M. Jaraiz, L. Pelaz, J. E. Rubio, J. Barbolla, G. H. Gilmer, D. J. Eaglesham, H.-J. Gossmann, and J. M. Poate, *Mater. Res. Soc. Symp. Proc.* **532**, 43 (1998).

¹⁶H. Bracht, E. E. Haller, and R. Clark-Phelps, *Phys. Rev. Lett.* **81**, 393 (1998).

¹⁷ $E_{\text{bind}} = 2.8 - 2.2[n^{1/2} - (n-1)^{1/2}]$ eV = 2.8 eV.

¹⁸P. A. Stolk *et al.*, *J. Appl. Phys.* **81**, 6031 (1997).

¹⁹N. E. B. Cowern, D. Alquier, M. Omri, A. Claverie, and A. Nejim, *Nucl. Instrum. Methods Phys. Res. B* **148**, 257 (1999).

²⁰B. Colombeau, F. Cristiano, A. Altibelli, C. Bonafos, G. Ben Assayag, and A. Claverie, *Appl. Phys. Lett.* **78**, 940 (2001).

²¹For example, Chap. 7 from D. R. Olander, *Fundamental Aspects of Nuclear Reactor Fuel Elements* (ERDA, Technical Information Center, Oak Ridge, Tenn, 1976).

²²C. S. Rafferty, G. H. Gilmer, M. Jaraiz, D. Eaglesham, and H.-J. Gossmann, *Appl. Phys. Lett.* **68**, 2395 (1996).

²³S. Takeda, *Jpn. J. Appl. Phys., Part 2* **30**, L639 (1991).

²⁴If clusters with different E_b were involved in the process, the Si interstitial supersaturation would change over time, but the total time integrated interstitial supersaturation would be independent of the binding energies of the intermediate stages.

²⁵If the surface were not a perfect sink, the effective distance to the surface would be $D+L$, being L the recombination length of the surface and D the actual distance to the surface.

²⁶M. Jaraiz, G. H. Gilmer, J. M. Poate, and T. D. de la Rubia, *Appl. Phys. Lett.* **68**, 409 (1996).

²⁷L. Pelaz, G. H. Gilmer, V. C. Venezia, H.-J. Gossmann, M. Jaraiz, and J. Barbolla, *Appl. Phys. Lett.* **74**, 2017 (1999).